REVISTA eIXO
revistaeixo.ifb.edu.br

ISSN 2238-5630
Brasília-DF, v. 15, n. 2, Maio - Agosto de 2026

MATHEMATICAL MODELING OF HYDRAULIC TRANSIENT APPLIED TO AN ADDUCTOR IN THE WEST OF SANTA CATARINA

MODELAGEM MATEMÁTICA DO TRANSIENTE HIDRÁULICO APLICADO A UMA ADUTORA NO OESTE DE SANTA CATARINA

Mauricio Bedin [1]
Rodrigo Konrath [2]
Keila Daiane Ferrari Orso [3]
Cristiano Reschke Lajús [4]

1. Graduado em Engenharia Mecânica pela Unidade Central de Educação Faem Faculdade (UCEFF)
E-mail: mauriciobedin-@hotmail.com
Lattes: https://lattes.cnpq.br/2434037438000286
ORCID: https://orcid.org/0009-0009-6094-9457

2. Mestre em Física pela Universidade Federal de Santa Catarina (UFSC)
Unidade Central de Educação Faem Faculdade (UCEFF)
E-mail: konrath@uceff.edu.br
Lattes: http://lattes.cnpq.br/9922756383272065

3. Mestra em Educação pela Universidade do Oeste de Santa Catarina (UNOESC)
Unidade Central de Educação Faem Faculdade (UCEFF)
E-mail: keilaorso@hotmail.com
Lattes: http://lattes.cnpq.br/6532350161899040
ORCID: https://orcid.org/0009-0009-5509-2532

4. Mestre e Doutor pela Universidade de Passo Fundo (UPF)
Universidade comunitária da região de Chapecó (Unochapecó)
E-mail: clajus@unochapeco.edu.br
Lattes: http://lattes.cnpq.br/8778314400284428
ORCID: https://orcid.org/0000-0003-3847-9793

ABSTRACT: The occurrence of perturbations in permanent flow inside penstocks induces shock waves due to pressure variations, a phenomenon known as a Hydraulic Transient. This condition generates internal stress in the fluid, which propagates to the pipe, affecting its operation and especially its safety. Additionally, the water hammer effect may occur, producing undesirable vibrations and noise. This study was conducted through a field investigation of an adductor in the West of Santa Catarina, aiming to mathematically model a transient flow caused by unexpected pump shutdowns, according to ABNT Standard 12215-1 (2017). The methodology included an analytical study using the Method of Characteristics and a computational analysis performed with ANSYS Fluent R19.2®, enabling comparison between both approaches. The results indicated discrepancies between analytical and computational outcomes at points with longer duct extensions, while convergence was observed in shorter sections. This finding demonstrates the validity of mathematical modeling while revealing its limitations in complex systems. The study concludes that analytical modeling remains useful for preliminary assessments, whereas CFD provides higher accuracy for critical sections. Future research should evaluate the performance of protective devices, such as hydropneumatics tanks, to mitigate transient effects and improve operational reliability.
Keywords: computational, analytical study; hydraulic transient; mathematical modeling; water hammer.

RESUMO: *A ocorrência de perturbações no escoamento permanente em condutos forçados induz ondas de choque devido à variação de pressão, fenômeno conhecido como Transiente Hidráulico. Essa condição gera tensões internas no fluido, propagadas para a tubulação, afetando seu funcionamento e especialmente sua segurança operacional. Além disso, pode ocorrer o efeito de Golpe de Aríete, produzindo ruídos e vibrações indesejáveis. Este estudo foi conduzido a partir de uma investigação de campo em uma adutora no Oeste de Santa Catarina, com o objetivo de modelar matematicamente um escoamento transiente provocado por paradas inesperadas da bomba, conforme a Norma ABNT NBR 12215-1 (2017). A metodologia envolveu um estudo analítico por meio do Método das Características e uma análise computacional utilizando o software ANSYS Fluent R19.2®, possibilitando a comparação entre os dois métodos. Os resultados indicaram discrepâncias entre os valores analíticos e computacionais em trechos de maior extensão do duto, enquanto houve convergência nos trechos menores. Esses achados demonstram a validade da modelagem matemática, ao mesmo tempo em que evidenciam suas limitações em sistemas mais complexos. Conclui-se que a modelagem analítica é útil para avaliações preliminares, enquanto a CFD oferece maior precisão em pontos críticos. Como perspectiva futura, sugere-se analisar o desempenho de dispositivos de proteção, como tanques hidropneumáticos, na atenuação dos efeitos transientes.*
Palavras-chave: estudo analítico-computacional; golpe de aríete; modelagem matemática; transiente hidráulico.

Recebido em: 02/07/2025
Aceito em: 16/10/2025

INTRODUCTION

Hydraulic systems consisting of pressure tubes, such as adductors, operate under broad and variable regimes. Any acceleration or deceleration of the flow leads to the propagation of pressure waves along the tube, producing a Hydraulic Transient, also known as the Water Hammer phenomenon. Situations in which flow conditions vary over time, or during the transition between two steady-state conditions, are referred to as transients. The greater and faster the change, the higher the transient pressure generated (TULLIS, 1989).

According to Chaudhry (1979), a Hydraulic Transient occurs, for example, when a valve is closed rapidly and the flow velocity suddenly decreases to zero, converting the kinetic energy of the steady flow into pressure energy. This increase in pressure propagates as pressure waves that travel and collide along the pipeline.

To reduce or prevent damages caused by this phenomenon, the Brazilian Association of Technical Standards (ABNT) established in Standard NBR 12215-1 (2017) the requirement to study the possibility of Water Hammer in water supply projects, using the Method of Characteristics (BRASIL, 2017). As highlighted by Chaudhry (1979), this method is a mathematical modeling technique applied to solve partial differential equations associated with the phenomenon.

The pipeline analyzed in this study connects a Water Treatment Plant (ETA) to a reservoir responsible for water distribution to the population. With a total length of approximately 1200 m, recently built, this adductor supplies treated water for human consumption. Given the essential demand, supply interruptions must be minimized, which increases the importance of operational safety.

When the flow is not properly controlled, or when systems lack effective anti-shock protection devices, the probability of transient events is very high. Their consequences can be severe and irreversible, leading to economic losses and risks to structural integrity.

In this context, the general objective of this work is to perform mathematical modeling to analyze the Hydraulic Transient in a real water supply system using the Method of Characteristics. The analysis first verifies whether working pressures comply with ABNT NBR 12215-1 (2017) and then establishes a computational model using ANSYS Fluent R19.2®, comparing the collected field data with the numerical method.

This study is guided by the following research question: Can the analytical modeling via the Method of Characteristics provide results comparable to Computational Fluid Dynamics (CFD) simulations for the analysis of Hydraulic Transients in adductors?

When the fluid flow is abruptly interrupted, velocity variations generate pressure wave shocks along the pipe. Such phenomena can cause intense vibrations and even pipe rupture, threatening both infrastructure and public safety. Therefore, modeling Hydraulic Transients is crucial in pipeline design, allowing the development of preventive measures and ensuring system reliability.

THEORETICAL REFERENCE

Hydraulic transient

Flow in hydraulic water distribution systems operates under different regimes. According to Amoah and Elbashir (2007), flow conditions are often regulated by valve operations or pump start-ups and shutdowns. A sudden valve closure or unexpected pump stop can trigger a Hydraulic Transient, producing abrupt changes in pressure and velocity.

Boulos *et al*. (2005) explain that rapid valve closure converts kinetic energy into pressure energy, generating pressure waves along the pipe. Part of this energy is also transformed into sound, characteristic of the Water Hammer effect, and dissipated through friction and other mechanisms. These energy losses gradually reduce wave intensity until the flow stabilizes again.

This dynamic behavior can be observed in the schematic presented in Figure 1, which illustrates the propagation of hydraulic transients at a given position (x) of the system. Recent studies reinforce the importance of this phenomenon. Martínez-Solano *et al*. (2020) highlight that hydraulic transient remain one of the main operational challenges in water supply systems due to their impact on service continuity and infrastructure integrity. More recently, Ghasemi and Karney (2021) reviewed advances in transient flow analysis, showing how modern simulation tools improve prediction of pressure surges and contribute to safer system design.

Figure 1 - Hydraulic Transient in (x) position of the system

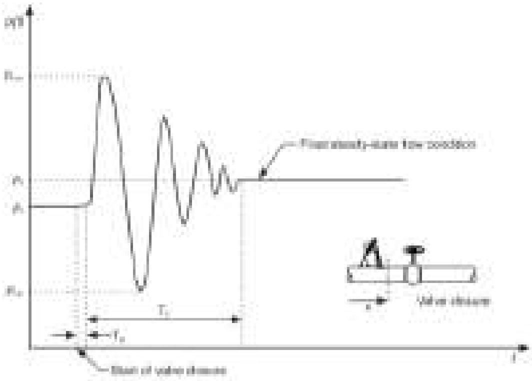

Source: Adapted from Beckeith, *et al*., (1992).

With variations in fluid flow, the system no longer remains in steady state. Initial conditions such as average velocity (v) and pressure (P) along the duct (x) vary with time (t) until the flow returns to steady conditions (AMOAH; ELBASHIR, 2007).

ISSN 2238-5630
Brasília-DF, v. 15, n. 2, Maio - Agosto de 2026

Mathematical modeling of the hydraulic transient

According to the methodology of Chaudhry (1979) and Wylie and Streeter (1979), the analytical solution of the Hydraulic Transient requires solving the Equation of Motion (Equation 1) and the Continuity Equation (Equation 2). These equations involve two dependent variables: piezometric head (H) and flow ($\dot{V}$) at a given position of the duct as a function of time.

$$\frac{d\dot{V}}{dt} ++ \frac{f\dot{V}|\dot{V}|}{2DA} = 0 \qquad (1)$$

$$\frac{\partial H}{\partial t} + \frac{a^2}{gA}\frac{\partial \dot{V}}{\partial x} = 0 \qquad (2)$$

Masiero Junior (2008) notes that these are nonlinear partial differential equations. Since they do not have closed-form analytical solutions, they are solved using numerical methods.

Flow velocity can be calculated from flow rate and duct area (Equation 3), and the flow regime can be classified by the Reynolds number (Equation 4).

$$\dot{V} = v \times A \qquad (3)$$

$$Re = \frac{\rho \times v \times D}{\mu} \qquad (4)$$

Where ρ is fluid density [kg/m³], v is velocity [m/s], D is pipe diameter [m], and μ is dynamic viscosity [N·s/m²].

The propagation of pressure waves along the pipeline is described by Equation 5 (BRASIL, 2017), which incorporates the elastic properties of water and pipe material:

$$a = \sqrt{\frac{\frac{K}{\rho}}{1+\frac{K}{E}\times\frac{DC}{e}}} \qquad (5)$$

Where K is the water bulk modulus [Pa], ρ is fluid density [kg/m³], E is pipe elasticity modulus [Pa], D is diameter [m], e is thickness [m], and C is a correction factor for pipe anchoring.

According to ABNT NBR 12215-1 (2017), the minimum pressure for steady flow must satisfy be $P_{min} \geq 50$ kPa. For transient flow, $P_{máx}$ should remain below the admissible pipe pressure, and P_{min} above atmospheric pressure.

Following Tullis (1989), Equations (1) and (2) are reformulated using the Method of Characteristics (MOC), resulting in the following characteristic equations:

$$L_1 = \frac{d\dot{V}}{dt} ++ \frac{f\dot{V}|\dot{V}|}{2DA} = 0 \qquad (6)$$

$$L_2 = \frac{\partial H}{\partial t} + \frac{a^2}{gA}\frac{\partial \dot{V}}{\partial x} = 0 \qquad (7)$$

By linear combination with a multiplier λ, we obtain:

$$L = L_1 + \lambda L_2 \qquad (8)$$

substituting terms:

$$\left[\frac{\partial \dot{V}}{\partial t} + \lambda a^2 \frac{\partial \dot{V}}{\partial x}\right]_I + \lambda + \frac{f\dot{V}|\dot{V}|}{2DA} = 0 \qquad (9)$$

This results in two real, non-zero values for λ, giving the positive and negative characteristic lines:

$$\frac{dx}{dt} = \lambda a^2 = \frac{1}{\lambda} = \lambda = \pm\frac{1}{a} \qquad (10)$$

along these lines, the compatibility equations are obtained:

$$\frac{d\dot{V}}{dt} + \frac{gA}{a}\frac{dH}{dt} + \frac{f\dot{V}|\dot{V}|}{2DA} = 0 \text{ Valid when, } \frac{dx}{dt} = a \qquad (11)$$

$$\frac{d\dot{V}}{dt} - \frac{gA}{a}\frac{dH}{dt} + \frac{f\dot{V}|\dot{V}|}{2DA} = 0 \text{ Valid when, } \frac{dx}{dt} =- a \qquad (12)$$

Figure 2 illustrates these positive and negative characteristic lines in the (x–t) plane, allowing visualization of transient propagation in time and space.

Figure 2 - Characteristic Line Chart

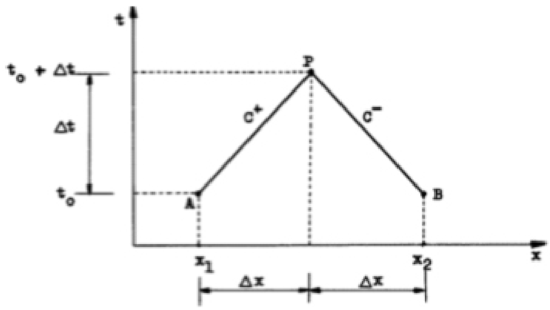

Source: Camargo (1991).

The Equation (11) represents the slope line (⅟a) 1a and Equation (12) represent the slope line (BP)(-⅟a), known as positive and negative characteristics lines.

When the conduit conditions are known in (A) (Figure 2) as($\dot{V}_A$, H_A, x_A e t_A), when ($t=t_0$). Thus, at the instant ($t=t_0+\Delta t$) are determined the conditions by a finite difference scheme called Equations of Compatibility (C^+) and (C^-). Multiplying Equation (11) and Equation (12) by (dt):

$$\int_A^P d\dot{V} + \frac{gA}{a}\int_A^P dH + \frac{f}{2DA}\int_A^P \dot{V}|\dot{V}|dt = 0 \qquad (13)$$

$$\int_B^P d\dot{V} - \frac{gA}{a}\int_B^P dH + \frac{f}{2DA}\int_B^P \dot{V}|\dot{V}|dt = 0 \qquad (14)$$

and performing the integration of (A) to (P) and (B) to (P), it gets:

$$C^+: \left(\dot{V}_P - \dot{V}_A\right) + \frac{gA}{a}\left(H_P - H_A\right) + \frac{f\Delta t}{2DA}\dot{V}_A\left|\dot{V}_A\right| = 0 \qquad (15)$$

$$C^-: \left(\dot{V}_P - \dot{V}_B\right) - \frac{gA}{a}\left(H_P - H_B\right) + \frac{f\Delta t}{2DA}\dot{V}_B\left|\dot{V}_B\right| = 0 \qquad (16)$$

these being the equations of the positive and negative characteristics lines.

It is considered (f) as the friction factor of the pipe, established first by the Miller Correlation (Equation 17) and then by the Colebrook Equation (Equation 18).

$$f_0 = 0,25\left[log\left(\frac{\frac{\varepsilon}{D}}{3,7} + \frac{5,74}{Re^{0,9}}\right)\right]^{-2} \qquad (17)$$

$$\frac{1}{\sqrt{f}} = -\ 2\log log\left(\frac{\frac{\varepsilon}{D}}{3,7} + \frac{2,51}{Re\sqrt{f}}\right) \qquad (18)$$

Finally, the elapsed time between two computational nodes is given by:

$$\Delta t = \frac{x}{v} \qquad (19)$$

where x is the distance step and v are the permanent flow velocity.

Recent contributions (Meniconi *et al*., 2020; Sun *et al*., 2022) have shown that integrating MOC with computational solvers increases accuracy and robustness in predicting pressure surges, particularly in long adductors where simplifications may accumulate errors.

Computational fluid dynamics (CFD)

The study of fluid dynamics has evolved significantly over the centuries. Initially, it was restricted to experimental investigations of fluid movement in pipes, known as hydraulics. With the subsequent introduction of mathematical expressions, links were established between dynamics and the forces acting on fluids, giving rise to hydrodynamics (FORTUNA, 2000).

The development of hydrodynamics advanced with Euler's formulation of the Equation of Motion, later expanded by Navier (1822), Poisson (1829), and Stokes (1845) into what is now known as the Navier–Stokes equations (SCHLICHTING, 1979). These equations describe the conservation of mass and momentum in fluid flows:

$$\nabla . u = 0 \qquad (20)$$

$$\rho(\frac{\partial u}{\partial t} + u \cdot \nabla u) = -\ \nabla p + \mu\nabla 2u + f \qquad (21)$$

where u is the velocity vector, ρ the fluid density, p the pressure, μ the dynamic viscosity, and f represents external forces such as gravity.

Pompeu (2010) emphasizes that analytical solutions of the Navier–Stokes equations are limited due to their nonlinear complexity, making numerical approaches necessary. Computational Fluid Dynamics (CFD) therefore begins with the formulation of a mathematical problem discretized into a computational grid, where governing equations are solved through iterative schemes (CHAPRA, 2013).

According to Fortuna (2000), the purpose of CFD is to reduce laboratory experiments and enable the analysis of phenomena that cannot be studied experimentally. In this context, CFD allows the evaluation of transient flow conditions, pressure wave propagation, and turbulence distribution, which are critical for validating the analytical method.

Recent contributions confirm its importance. Martínez-Solano *et al*. (2020) applied CFD to improve transient modeling in pressurized systems, while Sun *et al*. (2022) demonstrated that advanced turbulence models increase the accuracy of water hammer predictions. More recently, Zhang *et al*. (2023) highlighted the role of CFD in supporting design strategies to mitigate transients through protective devices. These studies reinforce the relevance of coupling CFD with classical analytical methods.

MATERIAL AND METHODS

Study site and pipeline characteristics

The field study was conducted on a pipeline operated by the Catarinense Company of Water and Sanitation (CASAN), which manages the public water supply system in Santa Catarina. During a technical visit in March 2019, it was identified that the pipeline operated at limited capacity due to the absence of the main anti-shock protection device, the hydropneumatics tank, in the discharge line. This condition motivated the present investigation to assess the fluid behavior in the adductor.

In August 2019, an analysis of the project drawings (CAD) was carried out with the company's civil engineering team. The discharge pipe was evaluated, consisting of approximately 1200 m in length, with a nominal diameter of 250 mm, internal diameter of 261.84 mm, and wall thickness of 6.08 mm, constructed in Fiberglass Reinforced Plastic (FRP). The line connects the Water Treatment Plant (ETA) to the elevated reservoir that distributes treated water to the city. The layout of the low- and high-zone system is presented in Figure 3.

ISSN 2238-5630
Brasília-DF, v. 15, n. 2, Maio - Agosto de 2026

Figure 3 - Water Supply System, low and high zone

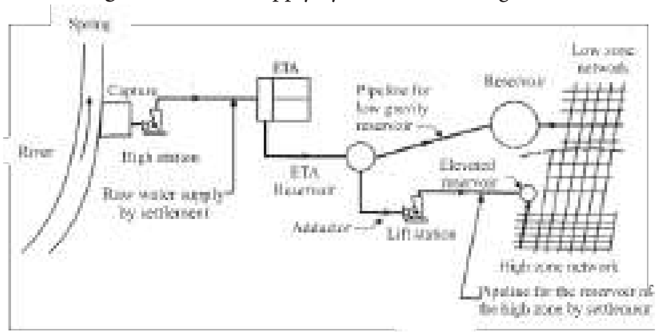

Source: Adapted from Tsutiya (2006).

Data collection

Data collection took place in October 2019, accompanied by CASAN's civil engineering team. A pressure gauge installed at the pump discharge line was used to measure the steady-state pressure. Terrain elevation differences were determined through a planialtimetric survey performed by a specialized company in western Santa Catarina. Pump flow data were obtained from CASAN's supervisory system, allowing calculation of permanent flow velocity (Equation 3).

The objective of the data collection was to characterize the hydraulic installation and establish boundary conditions for mathematical modeling and simulation.

Analytical modeling

Based on the collected data, mathematical modeling was performed using the Equation of Motion (Eq. 1) and the Continuity Equation (Eq. 2), in accordance with ABNT NBR 12215-1 (2017). These equations were applied through the Method of Characteristics (MOC) to derive the governing positive (Eq. 15) and negative (Eq. 16) characteristic line equations.

Computational modeling

In parallel, the pipeline was designed in SolidWorks 3D and exported for simulation in the computational fluid dynamics software ANSYS Fluent R19.2®, which provides results with high fidelity to real operating conditions.

Analytical and computational comparison

The study adopted a quantitative approach to analyze the pressure values, flow velocities, and wave propagation obtained through the analytical method (Eqs. 15 and 16) and CFD simulation. At the same time, a qualitative comparison was conducted to verify compliance with ABNT NBR 12215-1 (2017) and to evaluate the consistency between analytical and numerical results.

RESULTS AND DISCUSSIONS

Verification of permanent flow pressure

To ensure correct and reliable dimensioning of hydraulic water supply systems, ABNT NBR 12215-1 (2017) establishes maximum and minimum pressure conditions for both steady and transient flows. Since the analyzed system does not include the main protection against water hammer, the hydropneumatics tank. It was not possible to reproduce a hydraulic transient under field conditions for safety reasons. Nevertheless, the steady-state pressure was measured using a manometer installed at the pump discharge line. The measurement point is shown in Figure 4.

Figure 4 - Pressure gauge socket

Source: Research data (2019).

The measured steady-state pressure under normal conditions was approximately 114 m.c.a., subject to small variations. For comparison purposes, this value was converted into alternative units:

$$114\text{m.c.a.} \approx 11.4\text{bar} \approx 1117.2\text{kPa}$$

Thus, the discharge pipe operates in accordance with ABNT requirements, which stipulate a minimum pressure of $P_{min} \geq 50$ kPa. These results are consistent with findings from Martínez-Solano *et al.* (2020), who emphasize that maintaining pressures above the minimum threshold is crucial to prevent cavitation and ensure structural reliability in water distribution systems.

Geometric characterization of the adductor

For effective comparison between analytical and computational results, it was necessary to consider the terrain profile. Figure 5 presents the planialtimetric survey provided by a specialized company, representing the pipeline layout and its dimensions on a 1:3500 scale.

Figure 5 - Planialtimetric survey

Source: Adapted from Mediter (2019).

The adductor under study has a total length of 1200 m, a nominal diameter of 250 mm, an internal diameter of 261.84 mm, and a wall thickness of 6.08 mm, manufactured in Fiberglass Reinforced Plastic (FRP). The lowest point corresponds to the ETA (blue marker, 412 m elevation), while the highest point is the elevated reservoir (red marker, 555 m elevation), resulting in a total head difference of 143 m. Figure 6 illustrates the system elevations and extremities.

Flow and velocity determination

Using supervisory data from CASAN, the measured discharge flow was V = 0,058 m^3/s. Applying Equation 3, together with the pipe cross-sectional area, the velocity of permanent flow was determined as:

$$V = v \times A$$

$$0,058\ \frac{m^3}{s} = v \times \left(\frac{\pi \times (0,26184\ m)^2}{4}\right)$$

$$v = 1,074\ m/s$$

This velocity is consistent with values reported by Sun *et al*. (2022) in similar FRP pipelines, reinforcing the validity of the field measurements.

Analytical calculations

Based on the mathematical modeling described earlier and the collected field data, the analytical method was applied to determine wave speed, Reynolds number, and pipe friction factor. The parameters used are summarized in Table 1.

Table 1- Parameters used to calculate speed

Parameter	Value
K - Volumetric modulus of water elasticity	2,27x10 Pa
ρ - Specific mass of water	997 kg/m³
E - PRFV modulus of elasticity	10000 Pa
D - Duct diameter	0,26184 m
e - Duct thickness	6,08x m
ν - PRFV Poisson's ratio	0,3
C - Constant of how the pipe section is anchored	0,91
μ - Dynamic viscosity	0,89x N.s/m²

Source: Research data (2019).

The wave propagation speed was calculated using Equation (5):

$$a = \sqrt{\frac{\frac{K}{\rho}}{1+\frac{K}{E}\times\frac{DC}{e}}}$$

$$a = \sqrt{\frac{\frac{2,27\times10^{9}\ Pa}{997\ \frac{kg}{m^3}}}{1+\frac{2,27\times10^{9}\ Pa}{10000\ Pa}\times\frac{0,26184\ m\times0,91}{6,08\times10^{-3}\ m}}}$$

$$a = 0,51\frac{m}{s}$$

Next, the Reynolds number was determined from Equation (4):

$$Re = \frac{\rho \times v \times D}{\mu}$$

$$Re = \frac{997\ \frac{kg}{m^3}\times 1,074\ \frac{m}{s}\times 0,26184\ m}{0,89\times10^{-3}\ \frac{N.s}{m^2}}$$

$$Re = 314912$$

This result confirms a turbulent flow regime, consistent with values reported by Sun *et al.* (2022) in similar FRP adductors.

Friction factor estimation

The friction factor was initially estimated using the Miller correlation (Equation 17):

$$f_0 = 0,25[log(0,031 + 64,65\times10^{-6})]$$

$$f_0 = 0,015472$$

Subsequently, it was refined using the Colebrook equation (Equation 18), resulting in:

$$\frac{1}{\sqrt{f}} = -\ 2log\left(\frac{114,57\times10^{-3}}{3,7} + \frac{2,51}{4,87\times10^{3}}\right)$$

$$f_2 = 0,0155$$

where ε represents the pipe roughness provided by the manufacturer. The value obtained aligns with expected ranges for FRP pipes under turbulent conditions, corroborating observations by Meniconi *et al.* (2020).

ISSN 2238-5630
Brasília-DF, v. 15, n. 2, Maio - Agosto de 2026

Definition of simulation domain

With the constants defined, the positive and negative characteristic line equations (Eqs. 15 and 16) were applied to identify the system's critical points and prepare comparison with the computational model. To enable CFD simulations, the pipeline was first modeled in SolidWorks 3D, as shown in Figure 6, and later exported to ANSYS Fluent R19.2®.

Figure 6 - Isometric view of the pipeline

Source: Research data (2019).

For consistency between the methods, the adductor was divided into Points A to G, from ETA to the elevated reservoir. Table 2 presents the simulation parameters used in ANSYS Fluent R19.2®.

Table 2 - Simulation parameters

Parameter	Value
Pressure at ETA	1117,2 kPa
Initial velocity	1,074 m/s
Reservoir pressure	101,325 kPa

Source: Research data (2019).

Comparison of analytical and computational approaches

Using the compatibility equations (Eqs. 15 and 16), the intensity of turbulence at each point was calculated. For the section A–B, the analytical results were:

$$C^{+} = 3,18\frac{m^3}{s} \qquad C^{-} = -3,089\frac{m^3}{s}$$

These values indicate small variations in flow at the initial section, which were confirmed by CFD results. Figure 7 illustrates the velocity vectors for this section, showing limited disturbance and validating the analytical prediction.

Figure 7 - Speed vectors points A to B

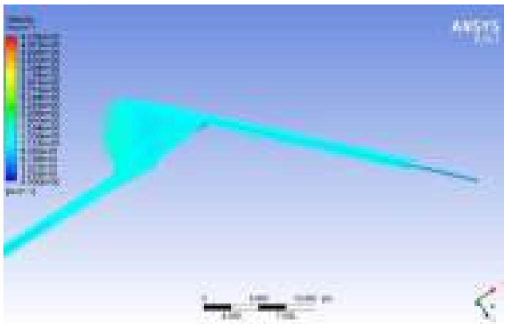

Source: Research data (2019).

At points B–C (Figure 6), the analytical method produced the following results:

$$C^{+} = 26,69\frac{m^3}{s} \qquad C^{-} = -25,51\frac{m^3}{s}$$

These results indicate moderate turbulence, consistent with the CFD simulation. Figure 8 illustrates the velocity vectors for this section, highlighting average turbulence across the pipe cross-section.

Figure 8 - Speed points B to C vectors

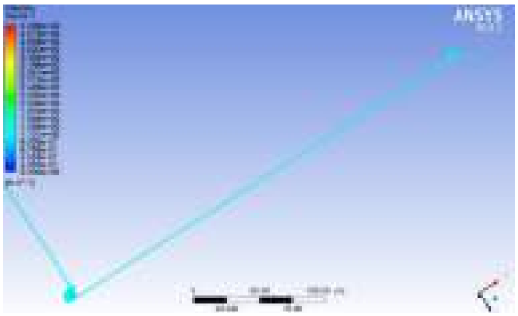

Source: Research data (2019).

In the longest section of the hydraulic system (C–D), the analytical method yielded:

$$C^{+} = 58,15\frac{m^3}{s} \qquad C^{-} = -56,71\frac{m^3}{s}$$

These values characterize this segment as a critical point, due to high turbulence and significant flow variation. Figure 9 confirms this behavior with large velocity vector fluctuations, indicating pressure instability.

Figure 9 - Velocity vectors points C to D

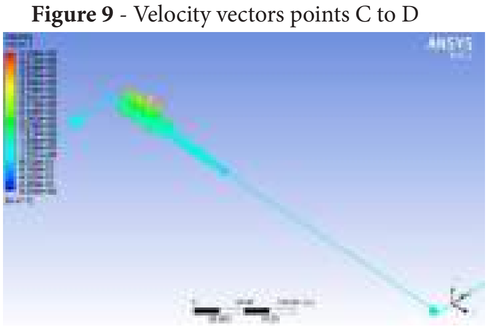

Source: Research data (2019).

For the short section D–E (Figure 6), the analytical method produced:

$$C^{+} = 2,26\frac{m^3}{s} \qquad C^{-} = -1,92\frac{m^3}{s}$$

These values indicate low flow variation, typical of short pipe stretches.

At section E–F, which mainly consists of a slope, the analytical results were inverted:

$$C^{+} = -1,92\frac{m^3}{s} \qquad C^{-} = 2,26\frac{m^3}{s}$$

This inversion reflects the effect of the slope on local flow dynamics. As shown in Figure 10, the velocity vectors shift orientation at Point E and subsequently stabilize along the slope.

Figure 10 - Velocity vectors points D to E and E to F

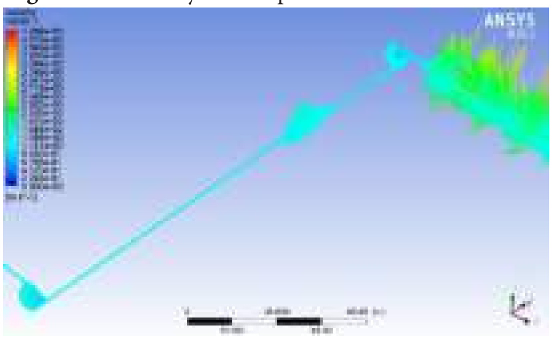

Source: Research data (2019).

These findings agree with Meniconi *et al.* (2020), who reported that local geometric variations, such as slopes and bends, cause temporary disturbances but tend to dissipate over short distances.

In the final section F–G, connecting to the elevated reservoir, the analytical method presented the highest flow variations:

$$C^{+} = 63,07\frac{m^3}{s} \qquad C^{-} = -62,23\frac{m^3}{s}$$

This section was identified as the most critical in terms of turbulence and instability. Figure 11 illustrates the large variation in velocity vectors, confirming the strong flow disturbance at this point.

Figure 11 - Speed vectors points F to G

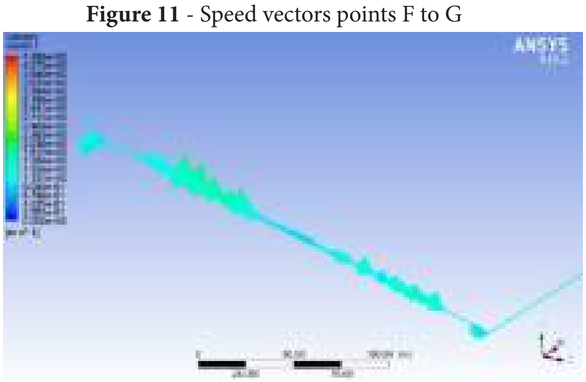

Source: Research data (2019).

This behavior is consistent with Ghasemi and Karney (2021), who highlight that reservoir inlets and outlets are among the most vulnerable areas for transient amplification, requiring special protective measures such as surge tanks or air chambers.

Numerical simulation results

As presented previously, the velocity variations analyzed along the system confirm that the flow is transient. According to Amoah and Elbashir (2007), under such conditions the average velocity (v) and pressure (p) vary with time (t) along the duct (x) until the flow returns to steady state.

The numerical simulation indicated a maximum flow velocity of v = 4.299 m/s, as shown by the red vectors in Figure 10. Using Equation (3) and the pipe cross-sectional area, the corresponding flow rate at points C–D was:

$$\dot{V} = v \times A \qquad \dot{V} = 4,290\frac{m}{s} \times \left(\frac{\pi \times (0,20104\ m)^2}{4}\right) \qquad \dot{V} = 0,231\frac{m^3}{s}$$

At points F–G, the simulation indicated a lower velocity of v = 3.168 m/s, yielding:

$$\dot{V} = v \times A \qquad \dot{V} = 3,168\frac{m}{s} \times \left(\frac{\pi \times (0,26184\ m)^2}{4}\right) \qquad \dot{V} = 0,171\frac{m^3}{s}$$

These results evidence discrepancies between analytical and computational methods, summarized in Table 3.

Table 3 - Confrontation of results, longest point and turbulence

	Points C to D	Points F to G
Analytical method	58,15 m³/s	63,07 m³/s
Computational method	0,231 m³/s	0,171 m³/s

Source: Research data (2019).

For shorter segments, such as A–B and D–E, the comparison was more favorable. Based on the CFD color gradient, the estimated velocities were approximately 1.584 m/s and 2.489 m/s, respectively. Applying Equation (3), the corresponding flow rates were:

$$\dot{V} = v \times A \qquad \dot{V} = 1,584\frac{m}{s} \times \left(\frac{\pi \times (0,26184\ m)^2}{4}\right) \qquad \dot{V} = 0,09\frac{m^3}{s}$$

$$\dot{V} = v \times A \qquad \dot{V} = 2,489\frac{m}{s} \times \left(\frac{\pi \times (0,26184\ m)^2}{4}\right) \qquad \dot{V} = 0,13\frac{m^3}{s}$$

The comparison between analytical and computational methods for these sections is presented in Table 4, showing greater convergence.

Table 4 - Confrontation of results, points with the shortest lengths

	Points A to B	Points D to E
Analytical method	3,18 m³/s	2,26 m³/s
Computational method	0,09 m³/s	0,13 m³/s

Source: Research data (2019).

This finding reinforces that the Method of Characteristics provides reliable results in shorter sections, while CFD is required for accurate predictions in long and highly turbulent stretches. Similar conclusions were reported by Ghasemi and Karney (2021), who highlighted the complementarity of analytical and numerical approaches.

Finally, it is important to note that, as stated by Fortuna (2000), CFD does not replace theoretical analysis, but it significantly reduces the time required for laborious calculations. Moreover, as emphasized by Miguez (2008), CFD is not free from errors and cannot fully substitute physical experiments. Therefore, combining analytical modeling, CFD simulations, and experimental validation remains the most robust strategy for studying hydraulic transients.

CONCLUSION

The study demonstrated that variations in velocity vectors along the adductor generated pressure changes characteristic of transient flow. The measured steady-state pressure at the pump discharge complied with ABNT NBR 12215-1 (2017), confirming the adequacy of operating conditions.

The analytical method, based on the Method of Characteristics, allowed the formulation of transient equations and provided consistent results for shorter sections of the pipeline. In contrast, the computational approach using ANSYS Fluent R19.2® refined the analysis in longer and more turbulent stretches, capturing localized instabilities with greater accuracy.

Although discrepancies were observed between the two methods, mainly due to simplifications in the analytical model, the overall comparison validated the mathematical modeling. This confirms that analytical modeling remains a useful tool for preliminary assessments, while CFD is essential for detailed analysis of complex systems.

As a practical contribution, the research highlights the sections most vulnerable to transients, providing technical support for preventive design measures.

For future work, it is recommended to perform simulations considering the installation of protective devices, such as hydropneumatics tanks, to evaluate their effectiveness in attenuating pressure waves and improving operational safety.

REFERENCES

AMOAH, S. O. K.; ELBASHIR, M. A. M. **Hydraulic Transient in a Pipeline Using Computer Model to Calculate and Simulate Transient.** Lund: Thesis (Master of Science) – Division of Water Resources, Department of Building and Environmental Technology, Lund University, 2007.

BECKEITH, S.; CHASE, D. V.; WALTER, G.; KOELLE, E.; SAVIC, D. A.; WALSKY, T. M. A**dvanced Water Distribution Modeling and Management.** 1. ed. Waterbury: Haestad Press, 1992.

BOULOS, P.; KARNEY, B.; LINGIREDDY, S.; WOOD, D. Hydraulic Transient Guidelines for Protecting Water Distribution Systems. **Journal AWWA**, v. 97, n. 5, p. 111-124, 2005.

BRASIL. *Associação Brasileira de Normas Técnicas.* ***NBR 12215-1:*** *Projeto de adutora de água para abastecimento público – Conduto forçado.* Rio de Janeiro, 2017.

CAMARGO, L. A. ***O Golpe de Aríete em Condutos – Análise pelo Método das Características.*** In: *XVI Encontro de Engenheiros de Assistência Técnica,* Joinville, n. 16, 1991.

CHAPRA, S. C. **Applied Numerical Methods with MATLAB for Engineers and Scientists**. 3. ed. Porto Alegre: McGraw-Hill, 2013.

CHAUDHRY, M. H. **Applied Hydraulic Transients**. New York: Van Nostrand Reinhold Company, 1979.

FORTUNA, A. O. ***Técnicas Computacionais para Dinâmica dos Fluidos.*** São Paulo: *Universidade de* São Paulo, 2000. *Disponível em:* https://books.google.com.br/books?id=J9CXhlB96skC. *Acesso em:* 20 abr. 2019.

GHASEMI, N.; KARNEY, B. Advances in Transient Flow Analysis in Water Distribution Systems: A Review. **Journal of Hydraulic Research**, v. 59, n. 6, p. 825-841, 2021. https://doi.org/10.1080/00221686.2020.1788550

MARTÍNEZ-SOLANO, F. J.; RAMÍREZ, F. J.; IGLESIAS-REY, P. L.; LÓPEZ-JIMÉNEZ, P. A. Hydraulic Transient Analysis in Pressurized Systems Using Computational Fluid Dynamics. **Water**, v. 12, n. 8, p. 2313, 2020. https://doi.org/10.3390/w12082313

MASIERO JUNIOR, A. ***Análise de Transientes Hidráulicos em uma Adutora Utilizando o Método das Características***. Florianópolis: *Projeto de Final de Curso – Universidade Federal de* Santa Catarina, 2008.

MEDITER. ***Mediter Serviços de Engenharia e Topografia LTDA***. Chapecó: [s.n.], 2019.

MENICONI, S.; BRUNONE, B.; MASSARI, C.; BERARDINELLI, A. In-Line Transient Tests for Pipeline System Characterization. **Journal of Hydraulic Engineering**, v. 146, n. 2, 2020. https://doi.org/10.1061/(ASCE)HY.1943-7900.0001686

MIGUEZ, F. ***Estudo em CFD do escoamento de líquido e da geração de área efetiva em recheios***. Rio de Janeiro: *Projeto de Final de Curso* – UFRJ/EQ, 2008.

POMPEU, R. C. ***Simulação Numérica e Visualização 3D Interativa de Objetos Sob Fluxos Irrotacionais em Tempo Quase-Real.*** *Tese (Doutorado em Mecânica Computacional) – Universidade Federal do* Paraná, Curitiba, 2010.

SANTOS, A. H.; CASTRO, A. H. ***Modelagem Computacional de Transientes Hidráulicos em Sistemas de Recalque***. In: I*V SEREA – Seminário Hispano-Brasileiro sobre Sistemas de Abastecimento Urbano de Água.* João Pessoa, 2004.

SCHLICHTING, H. **Boundary-Layer Theory**. 7. ed. New York: McGraw-Hill, 1979.

SUN, Y.; WANG, Z.; ZHANG, J.; ZHAO, J. Evaluation of Advanced Turbulence Models in Water Hammer Simulations. **Journal of Hydraulic Engineering**, v. 148, n. 4, 2022. https://doi.org/10.1061/(ASCE)HY.1943-7900.0002012

TSUTIYA, M. T. ***Abastecimento de Água***. 3. ed. São Paulo: *Departamento de Engenharia Hidráulica e Sanitária da Escola Politécnica da USP*, 2006.

TULLIS, J. P. **Hydraulics of Pipelines: Pumps, Valves, Cavitation, Transients**. Utah State: John Wiley & Sons, 1989.

WYLIE, E. B.; STREETER, V. L. **Fluid Transients.** New York: McGraw-Hill Book Company, 1979.

ZHANG, L.; LIU, Y.; WANG, J.; HUANG, Q. CFD-Based Design Strategies for Mitigating Hydraulic Transients in Pressurized Systems. **Journal of Hydraulic Research**, v. 61, n. 2, p. 145-159, 2023.